FOXM1 nuclear transcription factor translocates into mitochondria and inhibits oxidative phosphorylation

Markaisa Black[a,†], Paritha Arumugam[b,c,†], Samriddhi Shukla[a], Arun Pradhan[a,b], Vladimir Ustiyan[a,b], David Milewski[a], Vladimir V. Kalinichenko[a,b,d], and Tanya V. Kalin[a,b,*]

[a]Perinatal Institute and Division of Neonatology, Perinatal and Pulmonary Biology, [c]Translational Pulmonary Science Center and Division of Pulmonary Biology, and [d]Center for Lung Regenerative Medicine, Cincinnati Children's Hospital Medical Center, Cincinnati, OH 45229-3039; [b]Department of Pediatrics, University of Cincinnati College of Medicine, Cincinnati, OH 45267

ABSTRACT **Forkhead box M1 (FOXM1), a nuclear transcription factor that activates cell cycle regulatory genes, is highly expressed in a majority of human cancers. The function of FOXM1 independent of nuclear transcription is unknown. In the present study, we found the FOXM1 protein inside the mitochondria. Using site-directed mutagenesis, we generated FOXM1 mutant proteins that localized to distinct cellular compartments, uncoupling the nuclear and mitochondrial functions of FOXM1. Directing FOXM1 into the mitochondria decreased mitochondrial mass, membrane potential, respiration, and electron transport chain (ETC) activity. In mitochondria, the FOXM1 directly bound to and increased the pentatricopeptide repeat domain 1 (PTCD1) protein, a mitochondrial leucine-specific tRNA binding protein that inhibits leucine-rich ETC complexes. Mitochondrial FOXM1 did not change cellular proliferation. Thus, FOXM1 translocates into mitochondria and inhibits mitochondrial respiration by increasing PTCD1. We identify a new paradigm that FOXM1 regulates mitochondrial homeostasis in a process independent of nuclear transcription.**

Monitoring Editor
Thomas Fox
Cornell University

Received: Aug 1, 2019
Revised: Apr 17, 2020
Accepted: Apr 22, 2020

INTRODUCTION

Mitochondrial respiration is central to energy homeostasis and human health by serving as the cell's primary generator of ATP (Nunnari and Suomalainen, 2012). Because cellular energy needs vary depending on the function and activity of the cell, the precise coordination of energy production with physiological demand is essential. More than 90% of the energy produced by a cell depends

This article was published online ahead of print in MBoC in Press (http://www.molbiolcell.org/cgi/doi/10.1091/mbc.E19-07-0413) on April 29, 2020.

†These authors made equal contributions.

Conflict of interest: The authors have declared that no conflict of interest exists.

Author contributions: M.B. and T.V.K. conceived and designed the study. M.B., P.A., S.S., A.P., and D.M. performed the experiments. M.B., P.A., S.S., A.P., V.V.K., and T.V.K. analyzed and interpreted the data. M.B., P.A., and T.V.K. wrote the paper. All authors discussed the data. T.V.K. approved the submission of the manuscript.

*Address correspondence to: Tanya V. Kalin (Tatiana.kalin@cchmc.org).

Abbreviations used: APC/C-Cdh1, anaphase-promoting complex/cyclosome cadherin-1; Cdc25B, cell division cycle 25B; CMV, cytomegalovirus; CREB, cyclic-AMP response element binding protein; Cy, cytoplasmic; 3D, three-dimensional; DAPI, 4′,6-diamidino-2-phenylindole; DNA, deoxyribonucleic acid; DNase, deoxyribonuclease; ECAR, extracellular acidification rate; ERK, extracellular signal-regulated kinase; ETC, electron transport chain; FCCP, p-(trifluoromethoxy)phenylhydrazone; FOXM1, forkhead box M1; GFP, green fluorescent protein; IgG, immunoglobulin G; IP, immunoprecipitation; Leu, leucine; MEF2, myocyte enhancer factor 2; MEK, mitogen-activated protein kinase-extracellular signal-regulated kinase; MELAS, mitochondrial encephalopathy; Mi, mitochondrial; MLS, mitochondrial localization sequence; ΔMLS, mutated mitochondrial localization sequence; mRNA, messenger ribonucleic acid; Mt-tRNAs, mitochondrial transfer RNAs; MTATP6, mitochondrially encoded ATP synthase membrane subunit 6; MTCO1, cytochrome c oxidase subunit 1; MTG, mitotracker green, MTND1, mitochondrially encoded NADH:ubiquinone oxidoreductase core subunit 1; NF-κB, nuclear factor kappa-light-chain-enhancer of activated-B cells; NLS, nuclear localization sequence; Nu, nuclear; OCR, oxygen consumption rate; OXPHOS, oxidative phosphorylation; p53, transformation related protein 53; Plk1, Polo-like kinase 1; PRX3, peroxiredoxin 3; PTCD1, pentatricopeptide repeat domain 1; qRT-PCR, quantitative reverse transcription polymerase chain reaction; Raf, rapidly accelerated fibrosarcoma; SDHB, succinate dehydrogenase complex B; shRNA, short hairpin ribonucleic acid; siRNA, small interfering ribonucleic acid; STAT3, signal transducer and activator of transcription 3; TF, transcription factor; TMRM, tetramethylrhodamine methyl ester; TOP2, topoisomerase 2; UQCRC2, ubiquinol-cytochrome c reductase core protein 2; UTR, untranslated region; VDAC, voltage-dependent anion-selective channel 1.

on the electron transport chain (ETC) complexes or the process of oxidative phosphorylation (OXPHOS). Mitochondrial functions can be regulated by nuclear transcription factors (TFs) located in the mitochondria. Nuclear TFs regulate mitochondrial respiration by interacting with mitochondrial proteins or by binding to regulatory elements in mitochondrial DNA (Leigh-Brown *et al.*, 2010; Szczepanek *et al.*, 2012). These include nuclear factor kappa-light-chain-enhancer of activated B-cells (NF-κB), thyroid hormone receptor, cyclic-AMP response element binding protein (CREB), signal transducer and activator of transcription 3 (STAT3), myocyte enhancer factor 2 (MEF2), transformation-related protein 53 (p53), and estrogen receptor (Everts and Berdanier, 2002; Asin-Cayuela and Gustafsson, 2007; Wegrzyn *et al.*, 2009; Leigh-Brown *et al.*, 2010; She *et al.*, 2011; Szczepanek *et al.*, 2012). Understanding molecular mechanisms by which nuclear TFs regulate mitochondrial respiration addresses fundamental questions regarding the coordination of nuclear and mitochondrial functions.

In the present study, we have demonstrated a novel role of Forkhead box M1 (FOXM1) in regulating mitochondrial functions independently of nuclear gene transcription. Published studies demonstrated that FOXM1 directly regulates the transcription of cell cycle–associated genes, including Cdc25B, Cyclin B1, Plk1, TOP2, and Aurora B kinase, which are critical for G_1/S transition, mitosis, and DNA replication (Wang *et al.*, 2005). FOXM1 is one of the most common proto-oncogenes in solid tumors and is highly expressed in many human cancers (Teh *et al.*, 2002; Kalinichenko *et al.*, 2004; Costa *et al.*, 2005; Kalin *et al.*, 2011a; Wang *et al.*, 2014). Increased expression of FOXM1 in tumors is associated with advanced tumor stage with high proliferation rate and poor prognosis (Myatt and Lam, 2007; Wang *et al.*, 2008, 2012; Cai *et al.*, 2013). In transgenic mouse models, overexpression of FOXM1 increases growth and progression of lung, prostate, liver, colon, and breast cancers and glioma (Kalinichenko *et al.*, 2004; Kalin *et al.*, 2011b; Zhang *et al.*, 2008; Balli *et al.*, 2012; Wang *et al.*, 2012; Milewski *et al.*, 2017a). FOXM1 is activated by the RAF/MEK/ERK signaling pathway, which causes phosphorylation and translocation of FOXM1 into the nucleus and increased expression of cell cycle regulatory genes (Ma *et al.*, 2005; Weiler *et al.*, 2017). The transcriptional activity of FOXM1 is dependent on its phosphorylation, which increases at G_1/S and peaks during mitosis. At the end of mitosis, FOXM1 is poly-ubiquitinated and degraded via APC/C-Cdh1–mediated pathways (Park *et al.*, 2008). In addition to cellular proliferation, FOXM1 transcriptionally regulates genes critical for DNA repair, angiogenesis, surfactant production, estrogen signaling, and recruitment of inflammatory cells to injured tissues (Laoukili *et al.*, 2005; Kalin *et al.*, 2008b; Ren *et al.*, 2010; Balli *et al.*, 2011; Sun *et al.*, 2017; Shukla *et al.*, 2019). While FOXM1 is a powerful regulator of gene expression, other key functions of FOXM1 independent of nuclear transcription have not been identified.

We utilized confocal imaging, protein immunoprecipitation (IP), Seahorse Extracellular Flux (XF^e) technology, and Western blot analysis to demonstrate that FOXM1 is present in the mitochondria, where it acts as an inhibitor of mitochondrial respiration. Cells with FOXM1 targeted to the mitochondria had repressed mitochondrial function due to decreased membrane potential, oxygen consumption, and ETC activity. Mitochondrial FOXM1 bound to pentatricopeptide repeat domain protein 1 (PTCD1), a mitochondrial protein, negatively regulates mitochondrial leucine tRNAs. In sum, our present findings demonstrate that FOXM1 has a novel role in the regulation of mitochondrial functions where it decreases mitochondrial respiration independently from nuclear transcription.

RESULTS

FOXM1 nuclear transcription factor is found in the mitochondria and contains a mitochondrial localization sequence

FOXM1 has been characterized as a nuclear transcription factor (TF). However, in addition to nuclei, FOXM1 was detected throughout the cytoplasm in various human and mouse cell types (Supplemental Figure S1, top). Sequence analysis using the MitoProt computational program (Claros, 1995) showed that FOXM1 contains a highly conserved, N-terminal mitochondrial localization sequence (MLS) (Figure 1A). FOXM1 had a high probability to be imported into the mitochondria (human FOXM1 homologue: 0.9557; and mouse Foxm1 homologue: 0.7249; Figure 1A). FOXM1 partially colocalized with MitoTracker, a mitochondria-specific fluorescent dye, in several human and mouse cell lines (Figure 1B and Supplemental Figure S2A). The high-resolution three-dimensional (3D) confocal images demonstrated the specific localization of FOXM1 inside the mitochondria (Figure 1B, bottom panels). This suggests that FOXM1 may function in the mitochondria. To assess the distribution of FOXM1 in the cytoplasm and nucleus of NIH-3T3, A549, CCL-210, and HeLa cells, the intensity of FOXM1 fluorescence was quantified using CellProfiler software (Carpenter *et al.*, 2006). Approximately 60%–80% of FOXM1 was localized in the nucleus and 20%–40% in the cytoplasm (Supplemental Figure S2B). Treatment with leptomycin B increased nuclear localization of FOXM1 (Supplemental Figure S2, D and E). Western blot confirmed that FOXM1 was present in mitochondrial, cytoplasmic, and nuclear subcellular fractions (Figure 1, C and D and Supplemental Figure S2C). The purity of subcellular fractions was assessed using antibodies specific to mitochondrial (VDAC), cytoplasmic (β-TUBULIN), and nuclear (LAMIN A/C) proteins (Figure 1C and Supplemental Figure S2C). In mitochondrial fractions, FOXM1 was resistant to proteinase K treatment, which degrades proteins on the outer mitochondrial membrane (Figure 1E). STAT3, located in the inner mitochondrial membrane (Wegrzyn *et al.*, 2009), and PTCD1, a mitochondrial matrix protein, were also resistant to proteinase K treatment. VDAC, an outer mitochondrial membrane protein, was degraded by proteinase K (Figure 1E). All proteins were degraded after incubation with Triton X-100, which solubilizes the inner and outer membranes of the mitochondria (Wegrzyn *et al.*, 2009). Altogether, FOXM1 is present in the mitochondria and is localized within the mitochondria. These data support a role for FOXM1 in the mitochondria.

MLS is required for translocation of FOXM1 into the mitochondria

To study the functions of FOXM1 in the mitochondria, we used site-directed mutagenesis to generate two *FOXM1* cDNA constructs with different subcellular localization sequences. To inhibit localization of FOXM1 to the mitochondria, the FOXM1 MLS was mutated by substituting positively charged amino acids arginine (R) and lysine (K) with alanine (A) residues (Figure 2A). This construct, referred to as Δ*MLS-FOXM1*, has a low probability (0.08) of being imported into the mitochondria, as predicted by MitoProt (Figure 2A). To increase FOXM1 entry into the mitochondria, we fused *FOXM1* to the MLS of the *Cytochrome oxidase subunit VIII (COX VIII)* gene, which was successfully used to target several proteins to the mitochondria, including STAT3 transcription factor (Wegrzyn *et al.*, 2009; Laker *et al.*, 2014). This construct, referred to as *mitoFOXM1*, is predicted to have a high probability (0.99) of being imported into the mitochondria (Figure 2A). A wild-type *FOXM1 (FOXM1-FLAG)* construct was used as a control for normal

A

Species	Putative FOXM1 Mitochondrial Localization Sequence	Probability of Import to the Mitochondria
Human	MKTSPRRPLILKRRRLPLPVQNA	0.9557
Mouse	MRTSPRRPLILKRRRLPLPVQNA	0.7249
Rat	MRTSPRRPLILKRRRLPLPIQNA	0.7029
Xenopus Laveis	MRTSPRRPLILKRRKLSLPHQDA	0.9109
Danio Rerio	MRTSPRRPLILKRRRLPLPIQNA	0.7513

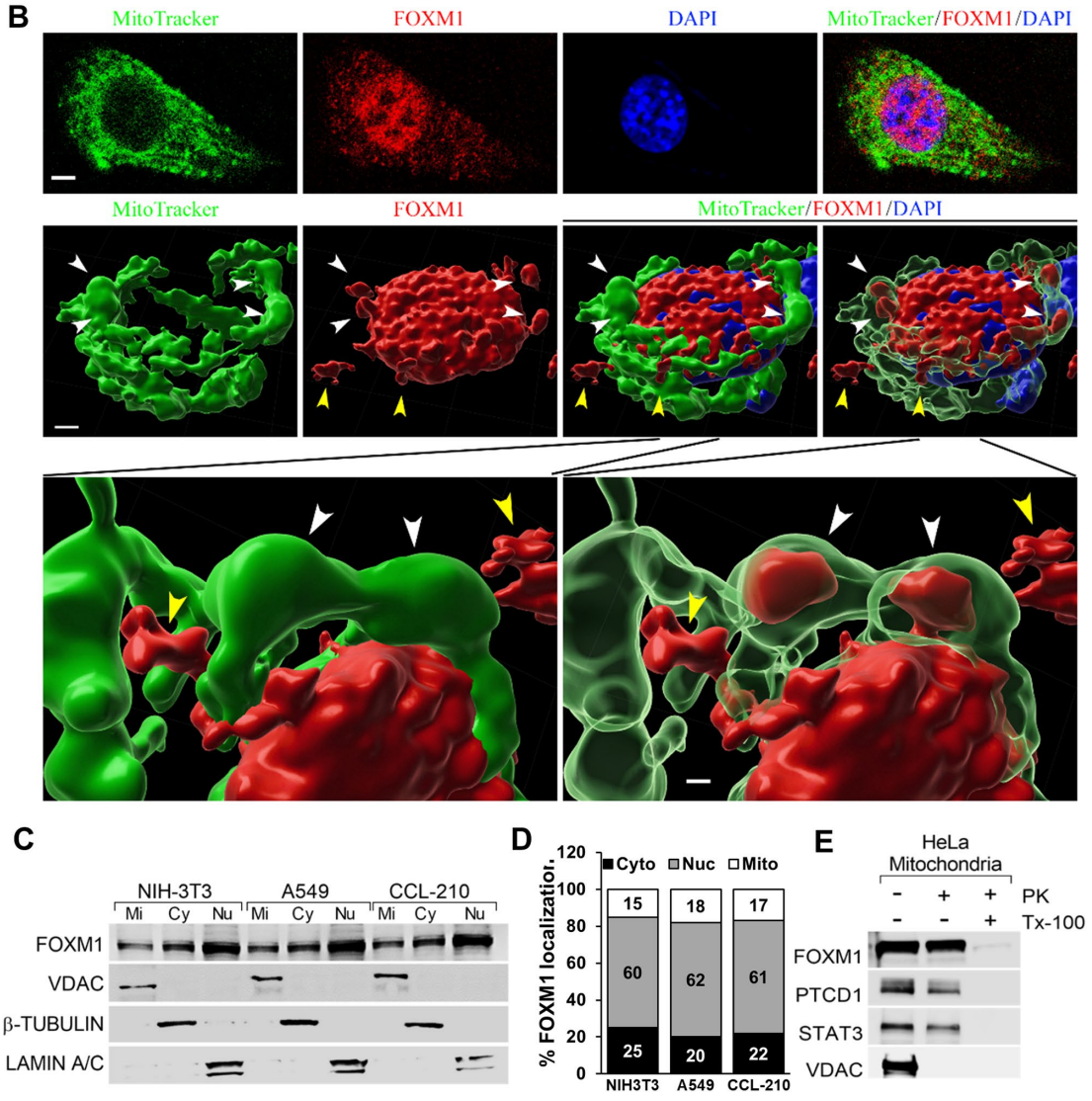

FIGURE 1: FOXM1 nuclear transcription factor is found in the mitochondria. (A) FOXM1 protein contains a highly conserved putative mitochondrial localization sequence (MLS). The MitoProt computational program predicted a positively charged (underlined) MLS in the N-terminus of FOXM1. FOXM1 MLS is highly conserved among several species (black font). Red color shows the differences compared with the MLS of human FOXM1. The probability of localization to the mitochondria for each FOXM1 orthologue was determined by MitoProt analysis. (B) Detection of FOXM1 in the mitochondria. High-resolution 3D confocal images show colocalization of FOXM1 (red) with mitochondrial marker MitoTracker (green) in NIH-3T3 cells. Nuclei were counterstained with DAPI. FOXM1 is present in the nucleus, mitochondria, and cytoplasm. White arrowheads point to the mitochondria with FOXM1 inside. Yellow arrowheads point to the cytoplasmic FOXM1. Magnification: ×100; 20 μm scale bar. (C) The presence of FOXM1 in mitochondrial (Mi), cytoplasmic (Cy), and nuclear (Nu) fractions is shown by Western blot with antibodies against FOXM1, VDAC (mitochondrial protein), β-TUBULIN (cytoplasmic protein), and LAMIN A/C (nuclear protein). (D) Quantification of FOXM1 protein levels in mitochondrial (Mi), cytoplasmic (Cy), and nuclear (Nu) fractions using densitometry. (E) Mitochondrial FOXM1 is proteinase K–resistant. Mitochondrial fraction was incubated without (lane 1) or with (lanes 2 and 3) 10 μg/ml proteinase K (PK). To disrupt mitochondrial integrity, 1% Triton X-100 (TX-100) was added in the digestion buffer (lane 3). Samples were probed for FOXM1, PTCD1 (mitochondrial matrix protein), STAT3 (inner membrane protein), and VDAC (mitochondrial outer membrane protein).

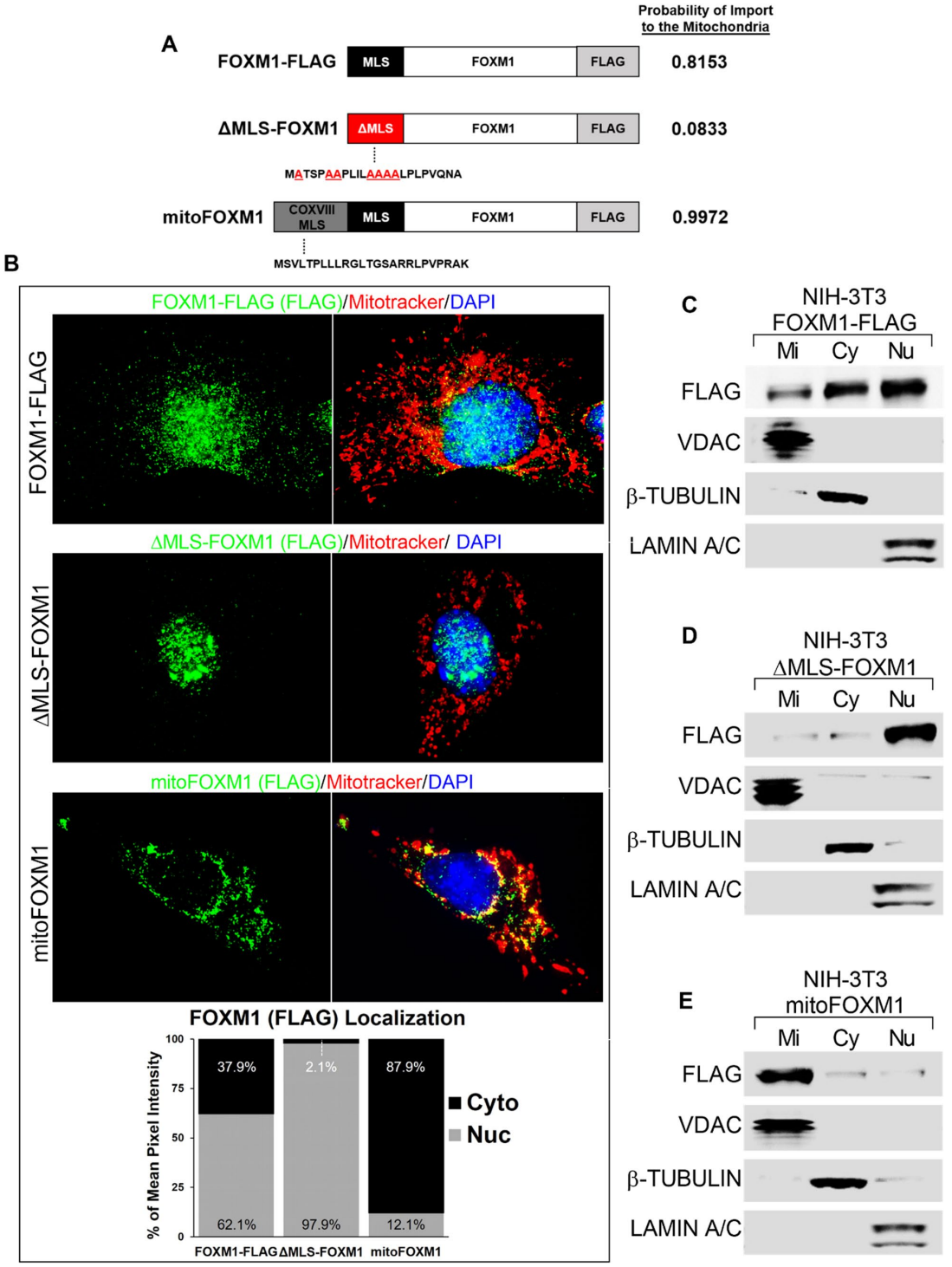

FIGURE 2: Mitochondrial localization sequence in FOXM1 is required for translocation of FOXM1 to mitochondria. (A) Schematic representation of FLAG-tagged FOXM1 protein constructs with wild-type MLS (black box), mutated MLS (red box), and COX VIII MLS fused to FOXM1 (gray–black box). The probability of each construct to be imported to the mitochondria was determined using MitoProt (Claros and Vincens, 1996). (B) Cellular localization of FLAG-tagged FOXM1 fusion proteins. NIH-3T3 cells transfected with *FOXM1-FLAG*, *ΔMLS-FOXM1*, or *mitoFOXM1* were used for colocalization studies with FLAG antibody (exogenous FOXM1) (green) and MitoTracker dye (red). Nuclei were counterstained with DAPI. Magnification: ×100; 20 μm scale bar. The intensity of FOXM1 fluorescence signal (green) in cytoplasmic (Cyto) and nuclear (Nuc) compartments was determined using CellProfiler software and is presented as the percent of mean pixel intensity (n = 7/group). (C–E) Western blots show the efficient localization of FOXM1 FLAG-tagged protein into different cellular compartments. NIH-3T3 cells expressing *FOXM1-FLAG* (C), *ΔMLS-FOXM1* (D), or *mitoFOXM1* (E) constructs were used to prepare mitochondrial (Mi), cytoplasmic (Cy), and nucleic (Nu) fractions. Western blots were probed with antibodies against FLAG (exogenous FOXM1), VDAC (mitochondrial protein), β-TUBULIN (cytoplasmic protein), and LAMIN A/C (nuclear protein).

distribution of FOXM1 (Figure 2A). All constructs contained a C-terminal FLAG tag to distinguish exogenous FOXM1 from endogenous FOXM1. Immunofluorescence and Western blot with FLAG antibodies showed that FOXM1-FLAG protein is present in the mitochondria, cytoplasm, and nucleus (Figure 2, B and C), similar to the distribution of endogenous FOXM1 (Figure 1, B and C). ΔMLS-FOXM1 was restricted to the nucleus (Figure 2, B and D), while mitoFOXM1 was detected primarily in the mitochondria and cytoplasm (Figure 2, B and E). Disruption of the endogenous nuclear localization sequence (NLS) with the retention of MLS of FOXM1 also led to mitochondrial localization of FOXM1 (Supplemental Figure S3). Inhibition of endogenous *FoxM1* by 3′UTR small interfering RNA (siRNA), ΔMLS-FOXM1 maintained nuclear localization, whereas mitoFOXM1 was still detected in mitochondria and cytoplasm (Supplemental Figure S4). Thus, ΔMLS-FOXM1 and mitoFOXM1 were specifically targeted to the nucleus and mitochondria, respectively.

FOXM1 inhibits mitochondrial membrane potential and regulates mitochondrial mass

To determine the role of FOXM1 in the regulation of mitochondrial function and content, we generated NIH-3T3 cell lines with stable overexpression *(OE FOXM1)* or short hairpin RNA (shRNA)-mediated knockdown of FOXM1 (*SH FOXM1)* (Supplemental Figure S5, A and B). Mitochondrial membrane potential (Δψm) was measured by flow cytometry analysis using tetramethylrhodamine methyl ester (TMRM) dye (Dingley *et al.*, 2012). We performed costaining with TMRM and MitoTracker green (MT) to assess membrane potential in MT green–stained cells. We observed a significant reduction in mitochondrial mass and membrane potential in FOXM1-overexpressing cells and a significant increase of mitochondrial mass and membrane potential in FOXM1-depleted cells compared with control cells (Figure 3, A and B, and Supplemental Figure S5C). The ratio of mitochondrial membrane potential to mitochondrial mass remained unaltered in FOXM1-overexpressing cells; knockdown of FOXM1 resulted in a significant decrease in the ratio of mitochondrial membrane potential to mitochondrial mass (Figure 3C). These findings show that FOXM1 inhibits mitochondrial membrane potential. To uncouple nuclear and mitochondrial functions of FOXM1, we transfected *FOXM1-FLAG, mitoFOXM1,* or Δ*MLS-FOXM1* constructs into *SH FOXM1* NIH-3T3 cells in which endogenous *FOXM1* was inhibited. Compared with control FOXM1-FLAG, mitochondrial mitoFOXM1 reduced Δψm, whereas nuclear ΔMLS-FOXM1 increased Δψm (Figure 3D). Altogether, translocation of FOXM1 into the mitochondria decreased mitochondrial mass and inhibited mitochondrial membrane potential.

Mitochondrial FOXM1 inhibits oxidative phosphorylation

To determine whether FOXM1 regulates mitochondrial respiration Seahorse XF^e analysis was used to measure the oxygen consumption rate (OCR), an indicator of mitochondrial respiration (Zhang *et al.*, 2012). We observed that knockdown of FOXM1 (*SH FOXM1*) increased OCR, whereas overexpression of FOXM1 (*OE FOXM1*) decreased OCR before oligomycin addition, suggesting the role of FOXM1 in regulating basal respiration (Figure 3E). Likewise, spare respiratory capacity (the difference between the maximum respiratory capacity after carbonyl cyanide *p*-(trifluoromethoxy) phenylhydrazone [FCCP] treatment and basal respiration) was increased in *SH FOXM1* cells but was undetectable in *OE FOXM1* cells (Figure 3E). Thus, FOXM1 inhibits mitochondrial respiration. In addition, overexpression of FOXM1 resulted in decreased nonmitochondrial respiration (Supplemental Figure 6, A and B). To determine whether the mitochondrial fraction of FOXM1 regulates respiration, we performed Seahorse XF^e assays using stable *SH FOXM1* cells transfected with *FOXM1-FLAG, mitoFOXM1,* or Δ*MLS-FOXM1* constructs. *mitoFOXM1* inhibited basal mitochondrial respiration and spare respiratory capacity compared with *FOXM1-FLAG* control (Figure 3F). In contrast, both basal respiration and spare respiratory capacity were significantly increased in Δ*MLS-FOXM1* cells (Figure 3F). Thus, the mitochondrial-specific FOXM1 fraction inhibits mitochondrial respiration. Finally, to determine whether FOXM1 affects glycolysis, we used Seahorse XF^e assays to examine the extracellular acidification rate (ECAR), an indicator of glycolysis (Brand and Nicholls, 2011). At basal levels, *OE FOXM1* increased ECAR, whereas *SH FOXM1* did not affect ECAR (Figure 3G). Both *mitoFOXM1* and Δ*MLS-FOXM1* significantly increased ECAR compared with *FOXM1-FLAG* control (Figure 3H), indicating that both mitochondrial and nuclear FOXM1 fractions regulate glycolysis.

Mitochondrial FOXM1 does not change cellular proliferation

FOXM1 induces cellular proliferation by translocating into the nucleus and activating transcription of cell cycle regulatory genes (Kalin *et al.*, 2011b). Therefore, we tested whether translocation of FOXM1 to the mitochondria influences cell proliferation. Endogenous FOXM1 levels were depleted in NIH-3T3 cells stably expressing *SH FOXM1*. Cell counts were compared between *SH FOXM1* cells transfected with *FOXM1-FLAG, mitoFOXM1,* or Δ*MLS-FOXM1* constructs. Expression of either wild-type FOXM1 (*FOXM1-FLAG*) or nuclear-restricted Δ*MLS-FOXM1* increased cell counts compared with *SH FOXM1* cells (Figure 4A), a finding consistent with the critical role of nuclear FOXM1 as a transcriptional activator of cell cycle regulatory genes (Kalinichenko and Kalin, 2015). In contrast to nuclear FOXM1 constructs, the total number of cells was unchanged after transfection of mitochondrial *mitoFOXM1* construct into *SH FOXM1* cells (Figure 4A). *MitoFOXM1* did not alter the cell cycle profile measured by DNA content (Figure 4, B and C). Thus, in contrast to nuclear FOXM1, the mitochondrial FOXM1 fraction does not stimulate cellular proliferation.

FOXM1 binds to mitochondrial matrix protein PTCD1

IP experiments using FLAG and FOXM1 antibodies demonstrated that FOXM1 physically bound to pentatricopeptide repeat domain 1 (PTCD1) (Figure 5, A and B). PTCD1 is a mitochondria-specific tRNA-binding protein that decreases mitochondrial leucine tRNAs that are critical to mitochondrial respiration (Rackham *et al.*, 2009; Schild *et al.*, 2014). To confirm the interaction of FOXM1 with PTCD1, reciprocal IP studies showed that FOXM1 protein was detected in PTCD1 immunoprecipitates (Figure 5, C and D). Treatment of protein lysates with proteinase K or DNase did not disrupt the binding of FOXM1 and PTCD1, suggesting that the FOXM1–PTCD1 interaction occurs within the mitochondria and is independent of DNA (Figure 5E). To validate that FOXM1 and PTCD1 bind and interact exclusively in the mitochondria, IP experiments were performed using nuclear and mitochondrial cell lysates. PTCD1 interacted with endogenous FOXM1 in the mitochondria, but not in nuclear lysates (Figure 5F). The purity of mitochondrial and nuclear fractions was confirmed using mitochondrial-specific VDAC protein and nuclear-specific LAMIN A/C proteins (Figure 5F). Thus, FOXM1 physically binds to PTCD1 in the mitochondria.

Because FOXM1 is a known transcriptional regulator (Kalin *et al.*, 2011b), we assessed whether FOXM1 regulates PTCD1 mRNA and protein. Depletion of FOXM1 (*SH FOXM1*) decreased PTCD1

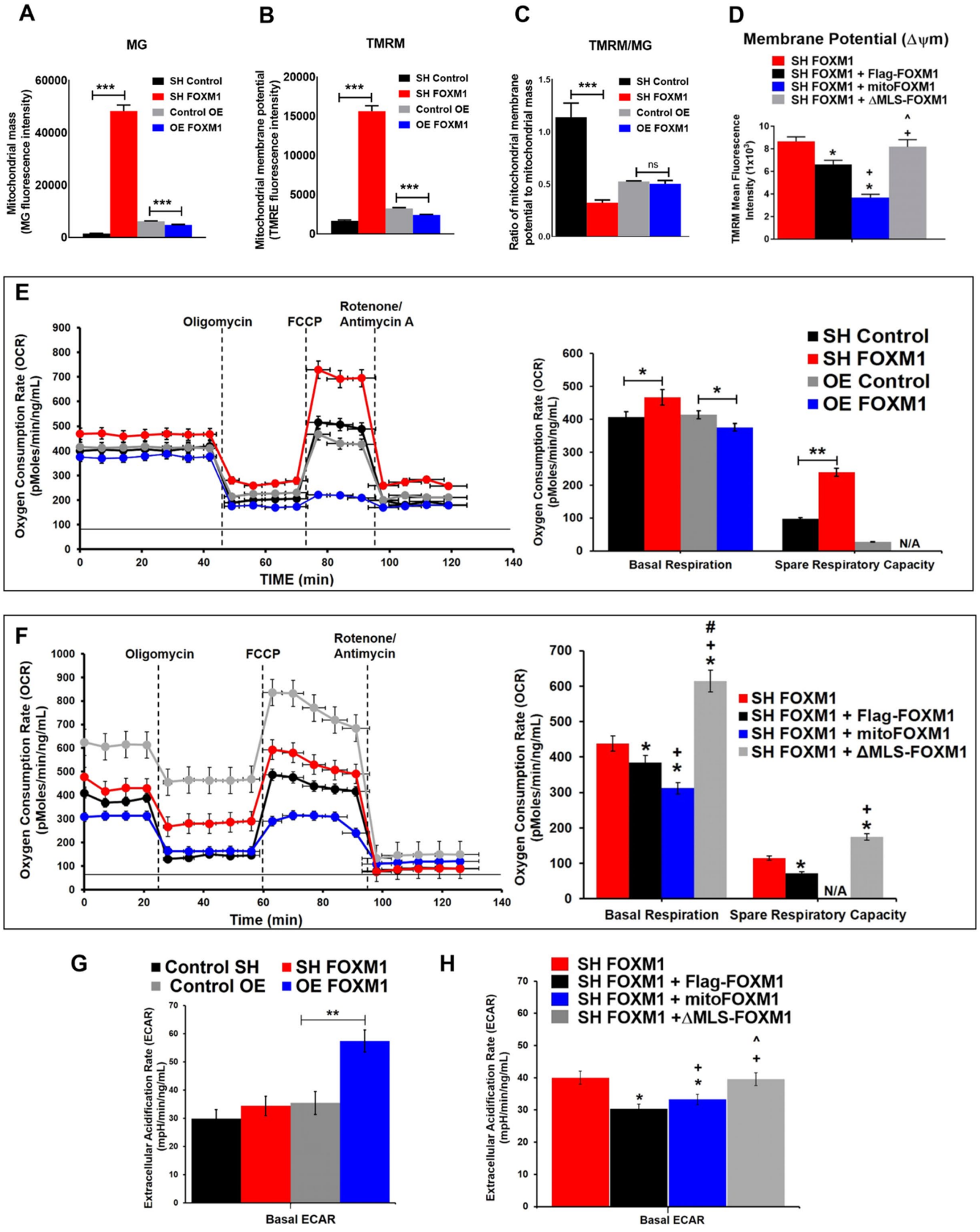

FIGURE 3: Mitochondrial FOXM1 inhibits mitochondrial membrane potential and oxidative phosphorylation. NIH-3T3 cells were costained with TMRM (mitochondria membrane potential) and MitoTracker green (MT, mitochondria mass) to assess membrane potential in MT green–stained cells using flow cytometry. (A) Loss of FOXM1 (*SH FOXM1* cells) increases mitochondrial mass; overexpression of FOXM1 (*OE FOXM1* cells) decreases mitochondrial mass. (B) Loss of FOXM1 increases mitochondrial membrane potential; overexpression of FOXM1 decreases mitochondrial membrane

protein levels, whereas overexpression of FOXM1 (*OE FOXM1*) increased PTCD1 protein (Figure 5G). FOXM1 did not affect *PTCD1* mRNA in three independent cell lines (Supplemental Figure S7, A and B), suggesting that FOXM1 regulates PTCD1 protein levels independently of *PTCD1* gene transcription. Consistent with these data, FOXM1 did not bind to the promoter region of the *PTCD1* gene as shown by chromatin IP (ChIP) sequencing (Supplemental Figure S8). FOXM1 directly bound to the *CDC25B* gene promoter (Supplemental Figure S8), a known transcriptional target of FOXM1 (Balli *et al*., 2013). Overexpression or knockdown of PTCD1 did not affect amounts of FOXM1 protein (Figure 5H). Altogether, FOXM1 binds to PTCD1 and increases its protein levels.

FOXM1 inhibits ETC complex proteins and activity

Published studies demonstrated that PTCD1 directly binds to and depletes leucine mitochondrial tRNAs, inhibiting the translation of mitochondrial-encoded proteins and suppressing oxidative phosphorylation in the mitochondria (Rackham *et al*., 2009; Schild *et al*., 2014). Because FOXM1 increases PTCD1, we assessed ETC complex proteins and the enzymatic activity of each complex in *SH FOXM1* and *OE FOXM1* cells. While overexpression of *FOXM1* significantly decreased both protein levels and activity of ETC complex I, II-III, and IV, inhibition of FOXM1 did not affect ETC complexes (Figure 6, A–C). To determine whether the mitochondrial fraction of FOXM1 regulates ETC complex proteins and the enzymatic activity of each complex, we used stable *SH FOXM1* cells transfected with *FOXM1-FLAG, mitoFOXM1,* or *ΔMLS-FOXM1* constructs. Interestingly, the *mitoFOXM1* significantly decreased ETC complex I, II, III, and IV protein levels and activity, while nuclear-restricted *ΔMLS-FOXM1* did not alter the protein levels or activity of ETC complexes (Figure 6, A, D, and E). To assess the impact of PTCD1 on ETC complexes and respiration, we generated PTCD1-depleted NIH 3T3 cells using a lentiviral vector expressing shPTCD1 from a minimal Cytomegalovirus promoter and carrying a turbo-GFP reporter. The activities of ETC complexes I, III, and IV were significantly decreased after PTCD1 knockdown (Supplemental Figure S9). Thus, mitochondrial FOXM1 inhibits ETC complexes I, II-III, and IV, a finding consistent with decreased mitochondrial respiration observed in *mitoFOXM1* cells (Figure 3F).

Our data demonstrate that mitochondrial FOXM1 directly binds to PTCD1, decreases activities of ETC complexes I, II-III, and IV, and inhibits mitochondrial respiration.

DISCUSSION

The transcriptional activities of FOXM1 are well-established; however, FOXM1 functions independent of nuclear transcription are poorly characterized. In this report, we demonstrate that FOXM1 protein is present in the mitochondria. The N-terminal region (MKTSPRRPLILKRRRLPLPVQNA) of FOXM1 is required for its import into the mitochondria, where it interacts with PTCD1 and inhibits mitochondrial respiration. A previous study found that peroxiredoxin 3 (PRX3), a mitochondrial matrix antioxidant enzyme, colocalized with FOXM1 in human malignant mesothelioma (Cunniff *et al*., 2013). Although previous reports implicated FOXM1 in regulation of oxidative stress and in the generation of reactive oxygen species (Park *et al*., 2009), these functions of FOXM1 were mediated by its role in transcription. In the present study, we generated mitochondrial- and nuclear-specific FOXM1 targeting proteins to uncouple nuclear and mitochondrial functions of FOXM1.

Cell proliferation and respiration are coordinated to maintain the energy needed during cell growth (Vander Heiden *et al*., 2009). FOXM1 is a transcriptional regulator of cell cycle–associated genes (Laoukili *et al*., 2005; Wang *et al*., 2012). Consistent with previous studies, we found that nuclear FOXM1, but not mitochondrial FOXM1, increased cell proliferation. This supports the concept that FOXM1 stimulates cell proliferation via its nuclear, but not mitochondrial, activity. ECAR, an indicator of glycolysis, increased in cells expressing either mitochondrial FOXM1 or nuclear FOXM1, suggesting that FOXM1 promotes glycolysis via multiple mechanisms.

potential. (C) The ratio of mitochondrial membrane potential to mitochondrial mass is decreased in FOXM1-depleted cells and is unchanged in FOXM1-overexpressing cells compared with control mock-transduced cells. (D) Mitochondrial FOXM1 inhibits mitochondrial membrane potential. NIH-3T3 cells stably expressing *SH FOXM1* were transiently transfected with *FOXM1-FLAG, ΔMLS-FOXM1,* or *mitoFOXM1*. Tetramethylrhodamine methyl ester (TMRM) dye that accumulates in active mitochondria with intact membrane potentials was used to stain cells and analyzed by flow cytometry. MFI, mean fluorescence intensity. Data represent mean ± SEM from experiments in triplicate. * indicates statistical significance of $p < 0.05$ compared with SH FOXM1. + indicates statistical significance of $p < 0.05$ compared with SH FOXM1 + FLAG-FOXM1. ^ indicates statistical significance of $p < 0.05$ compared with SH FOXM1 + mitoFOXM1. (E) Mitochondrial respiration measured by Seahorse XF^e assay in NIH-3T3 cell lines with stable overexpression or knockdown of FOXM1. The oxygen consumption rate (OCR, pmol/min/ng/ml) was decreased in response to overexpression of FOXM1, and increased in response to knockdown of FOXM1 compared with controls. Graphs represent data from five independent experiments. (F) Mitochondrial FOXM1 inhibits oxidative phosphorylation. NIH-3T3 cells stably expressing *SH FOXM1* were transiently transfected with indicated constructs. Red dotted line represents OCR values from NIH-3T3 cells stably expressing *SH FOXM1* only. Mitochondrial oxygen consumption rate (OCR, pmol/min/ng/ml) was measured under basal conditions and in response to modulators of the electron transport chain. Graphs represent data from four replicate experiments. Data represent mean±SEM, $n = 4$, ANOVA, Bonferroni's post test. * indicates statistical significance of $p < 0.05$ compared with SH FOXM1. + indicates statistical significance of $p < 0.05$ compared with SH FOXM1 + FLAG-FOXM1. #indicates statistical significance of $p < 0.05$ compared with SH FOXM1 + mitoFOXM1. (G) Stable overexpression of FOXM1 increased glycolysis. Under basal conditions, the extracellular acidification rate (ECAR, mpH/min/ng/m[), a readout for glycolysis, is directly correlated with FOXM1 levels. Graphs represent data from five replicate experiments (mean±SEM, $n = 5$, ANOVA, Bonferroni's post test, **$p < 0.01$ indicates statistical significance. (H) Mitochondrial and nuclear FOXM1 increased glycolysis shown by increased ECAR. NIH-3T3 cells stably expressing *SH FOXM1* were transiently transfected with the indicated constructs. ECAR was increased in MLS FOXM1 mutants compared with *FLAG-FOXM1* expressing cells. Graphs represent data from four replicate experiments. Data represent mean±SEM, $n = 5$, ANOVA, Bonferroni's post test. * indicates statistical significance of $p < 0.05$ compared with SH FOXM1. + indicates statistical significance of $p < 0.05$ compared with SH FOXM1 + FLAG-FOXM1. ^ indicates statistical significance of $p < 0.05$ compared with SH FOXM1 + mitoFOXM1.

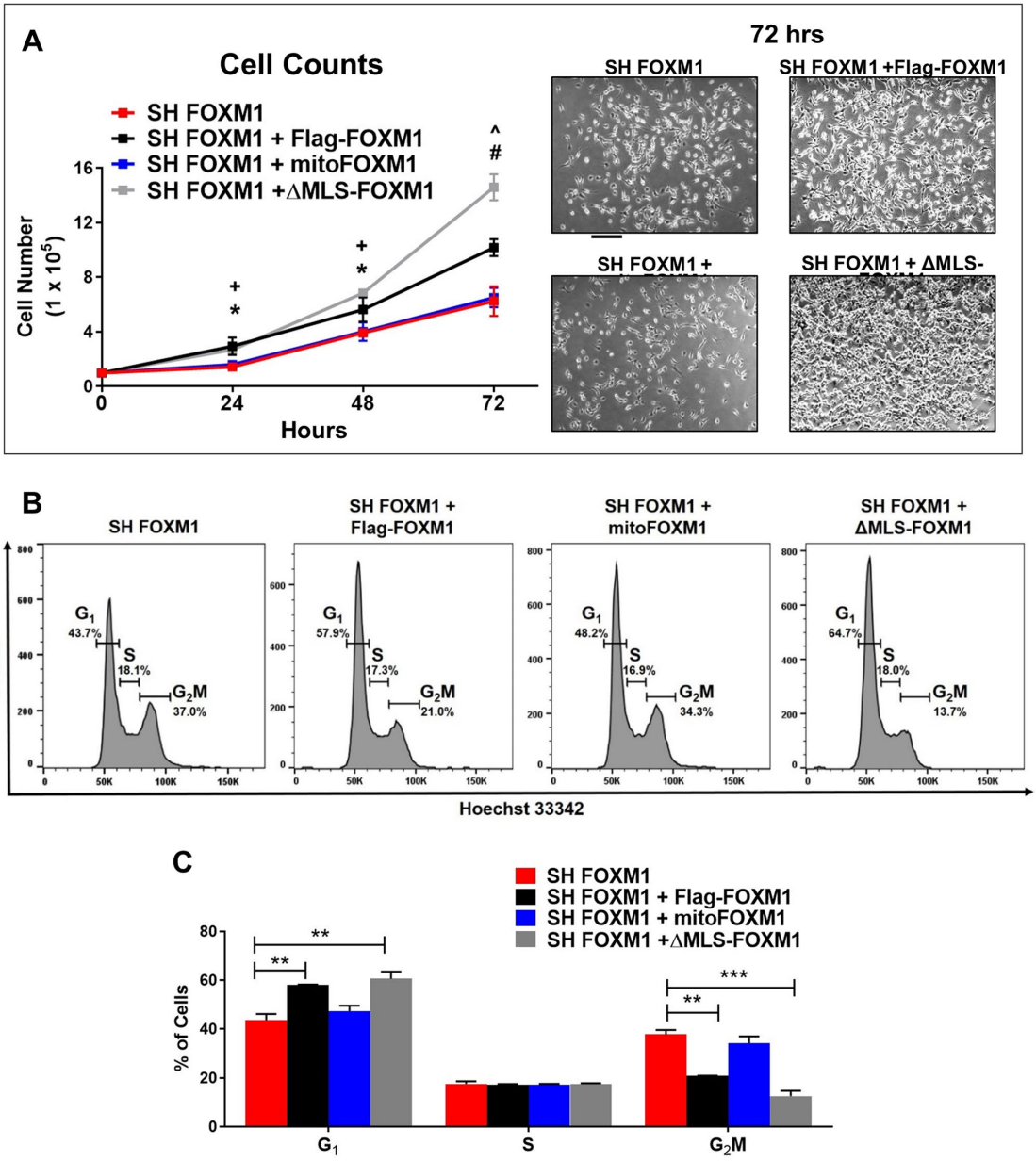

FIGURE 4: Translocation of FOXM1 to the mitochondria does not affect proliferation. (A) Growth curves of *SH FOXM1* cells transfected with *FLAG-FOXM1, mitoFOXM1, or ΔMLS-FOXM1* constructs. Cells were counted at 24, 48, and 72 h. Representative images are shown for each group at 72 h. Magnification: ×5; 100 μm scale bar. Graph represents data from $n = 5$ replicates presented as mean±SEM, $n = 5$, ANOVA, Bonferroni's post test. * indicates statistical significance of $p < 0.05$ comparing SH FOXM1 + Flag-FOXM1 to SH FOXM1. + indicates statistical significance of $p < 0.05$ comparing SH FOXM1 + ΔMLS-FOXM1 to SH FOXM1. #indicates statistical significance of $p < 0.001$ comparing SH FOXM1 + ΔMLS-FOXM1 to SH FOXM1. ^ indicates statistical significance of $p < 0.001$ comparing SH FOXM1 + Flag-FOXM1 to SH FOXM1. (B) Effects of FOXM1 localization on cell cycle distribution. *SH FOXM1* cells were transfected with the indicated MLS mutant constructs, and cell cycle analysis was measured using Hoechst 3342 and flow cytometry 72 h post–serum starvation. (C) Representative quantitative chart depicts cell cycle phase. Graph represents G1, S, and G2/M phases and values are presented as mean ± SEM from four replicates. Red dotted line represents OCR values from NIH-3T3 cells stably expressing *SH FOXM1* alone. Statistical significance is indicated with an asterisk (*); *$p < 0.05$, **$p < 0.01$, and ***$p < 0.001$.

This is consistent with published studies demonstrating that FOXM1 transcriptionally activates genes important for glycolysis (Cui *et al.*, 2014). Further, since mitochondrial FOXM1 suppressed mitochondrial respiration, increased glycolysis may act as a compensatory mechanism to meet cellular energy demands (Vander Heiden *et al.*, 2009). Collectively, the present data suggest that FOXM1 is a critical mediator of cellular bioenergetics.

Several diseases are linked to dysfunctional mitochondrial activity caused by abnormal mt-tRNA levels, including mitochondrial myopathy, encephalomyopathy, lactic acidosis, and stroke-like episodes (MELAS) (Suzuki *et al.*, 2011). A recent study identified PTCD1, a mt-tRNA–binding protein, as a possible mitochondrial disease gene associated with deficiencies in mitochondrial respiratory chain complexes (Taylor *et al.*, 2014). The present findings

demonstrate that FOXM1 binds to PTCD1 protein in the mitochondria. Inhibition of FOXM1 by siRNA decreased the steady-state levels of PTCD1 protein but did not affect *PTCD1* mRNA. Thus, it is possible that FOXM1–PTCD1 protein–protein interactions are important for the stability of PTCD1 protein. PTCD1 binds to mitochondrial leucine tRNAs and was regulated by leucine deprivation (Schild *et al.*, 2014); it is possible that FOXM1 stabilizes PTCD1 in the mitochondria, which in turn regulates leucine mt-tRNAs.

PTCD1 is a pentatricopeptide repeat (PPR) domain protein that serves as an RNA-binding protein (Perks *et al.*, 2018). Several PPR domain proteins regulate mitochondrial function by various mechanisms including transcription of mitochondrial DNA, processing mt-RNAs and by associating with mitochondrial ribosomal subunits (Falkenberg *et al.*, 2007; Davies *et al.*, 2012). PTCD1 is required for 16S rRNA maturation complex stability and mitochondrial ribosome assembly (Perks *et al.*, 2018). PTCD1 binds to and decreases mitochondrial transfer RNAs (mt-tRNA) $Leu^{(CUN)}$ and mt-tRNA $Leu^{(UUR)}$ levels. Low levels of leucine mt-tRNAs inhibit ETC complexes I and IV, which contain subunits with the highest overall leucine content (Rackham *et al.*, 2009; Schild *et al.*, 2014). Our results are consistent with previous studies that show inhibition of PTCD1 increased ETC complex protein levels and activity (Rackham *et al.*, 2009; Schild *et al.*, 2014). These studies support our findings that FOXM1 suppressed ETC activity and mitochondrial respiration, at least in part, via PTCD1, regulating leucine mt-tRNAs in the mitochondria.

In addition to inhibiting leucine-rich ETC complexes I and IV, FOXM1 decreased protein levels and activity of ETC complexes II and III. This supports the concept that mitochondrial FOXM1 has diverse functions that may contribute to the regulation of ETC proteins and complex activity beyond PTCD1-mediated pathways. Several nuclear TFs translocate to the mitochondria and affect mitochondrial respiration via protein–protein interactions or by regulating mitochondrial gene expression (Szczepanek *et al.*, 2012). For example, STAT3 increased ETC activity of complexes I and II by binding to GRIM-19 (Wegrzyn *et al.*, 2009) and increased mitochondrial encoded genes as a mitochondrial TF (Carbognin *et al.*, 2016). Because FOXM1 directly binds to STAT3 in the nucleus (Maachani *et al.*, 2016), it is possible that FOXM1 and STAT3 also interact in the mitochondria. Therefore, FOXM1 may regulate ETC complex activities and mitochondrial respiration through regulation of STAT3.

In summary, FOXM1 translocates into the mitochondria, inhibits mitochondrial respiration, and interacts with PTCD1, which is critical for regulation of mitochondrial leucine tRNAs. FOXM1 has a role independent of nuclear transcription and may be a promising molecular target to modulate mitochondrial respiration.

MATERIALS AND METHODS

Mitochondrial and subcellular fractionation

Mitochondrial, cytoplasmic and nuclear lysates were isolated by standard differential centrifugation (Frezza *et al.*, 2007). Briefly, cells were trypsinized, washed in phosphate-buffered saline (PBS), and collected at 600 × *g* at 4°C in ice-cold mitochondrial isolation buffer. Cells were manually homogenized using a glass pestle in a glass potter and centrifuged at 600 × *g* for 10 min at 4°C. Supernatant was centrifuged at 7000 × *g* for 10 min at 4°C. The supernatant (cytoplasmic fraction) was collected. The pellet (mitochondrial fraction) was washed in 200 µl of ice-cold isolation buffer and centrifuged at 7000 × *g* for 10 min at 4°C. The mitochondrial fraction was suspended in 50 µl of mitochondrial isolation buffer. All fractions were measured for protein concentration using the Bradford assay (Bio-Rad). Nuclear and cytoplasmic fractions were processed using standard lysis buffer (Pradhan *et al.*, 2016).

In silico analysis

The protein sequences for Foxm1 from *Homo sapiens* (human), *Mus musculus* (mouse), *Rattus norvegicus* (rat), *Xenopus laevis* (frog), and *Danio rerio* (zebrafish) were downloaded from the NCBI protein database (http://www.ncbi.nlm.nih.gov/protein/). Sequence alignments were generated using Clustal Omega (Sievers *et al.*, 2011). The MitoProt (Version 8.0) computational program was used to identify putative mitochondrial localization sequences and the probability of localization to the mitochondria for Foxm1 protein sequence listed above (Claros, 1995).

Western blot

Protein extracts for Western blot were prepared from cells using lysis buffer or mitochondrial isolation buffer (Frezza *et al.*, 2007; Cheng *et al.*, 2014; Pradhan *et al.*, 2016). Western blot analysis was done as previously described (Cheng *et al.*, 2014; Milewski *et al.*, 2017b). The indicated lysates were incubated with 10 µg/ml proteinase K (PK) or DNase for 30 min. A complete primary antibody list is given in Supplemental Table 1. ACTIN or PORIN (VDAC) were used as loading controls. The signals from the primary antibody were enhanced by horseradish peroxidase–conjugated IgG (Bio-Rad) and detected with a Pierce ECL Western blotting substrate (Thermo Scientific) followed by autoradiography.

Quantitative real-time reverse transcription-PCR

The RNeasy Mini kit (Qiagen) was used to isolate total RNA from lysates. mRNAs of specific genes were analyzed by quantitative reverse transcription-PCR using the StepOnePlus Real-Time PCR system (Applied Biosystems) as previously described (Cheng *et al.*, 2014; Cai *et al.*, 2016; Milewski *et al.*, 2017b). The TaqMan probes used are listed in Supplemental Table 2.

Immunoprecipitation

IP experiments were performed from mitochondrial or total cell extracts by using the Mitochondrial Protein Immunoprecipitation Kit (Sigma) or a two-step affinity chromatography protocol as described previously (Pradhan *et al.*, 2016; Shukla *et al.*, 2019). The indicated lysates were incubated with 10 µg/ml proteinase K (PK) or DNase for 30 min. For total extracts, cells expressing FLAG-FOXM1 were washed with PBS and collected as a pellet. The first purification step included the incubation of total lysates with anti-FLAG M2 agarose beads (Sigma) followed by elution with 3xFLAG peptide. The second purification step was performed by incubating the 3xFLAG peptide eluate with Talon metal affinity resin (BD Biosciences) in the presence of 3 mM imidazole. Bound proteins were eluted using 2x sample buffer. For mitochondrial IP, mitochondria were solubilized in Mitochondria Protein IP Buffer (catalogue number MTP001A) and centrifuged at 12,000 × *g* for 10 min at 4°C. Immunoglobulin G (IgG) (Vector Lab), FLAG, FOXM1, or PTCD1 antibody was incubated in the solubilized mitochondrial supernatant overnight at 4°C. IP proteins were eluted in SDS–PAGE gel loading buffer. Purified proteins were resolved on SDS–PAGE gel and analyzed by immunoblotting.

Generation of mitoFOXM1 and ΔMLS-FOXM1 constructs and transfection studies

To generate constructs that localize FOXM1 specifically to the mitochondria (mitoFOXM1), the mitochondrial localization sequence (MLS) from cytochrome *c* oxidase subunit VIII containing *Nhe*I and *Eco*RV restriction sites on the 5′and 3′ ends, respectively, was cloned into the mouse pcDNA3.1+-DYK-FOXM1 vector (GenScript).

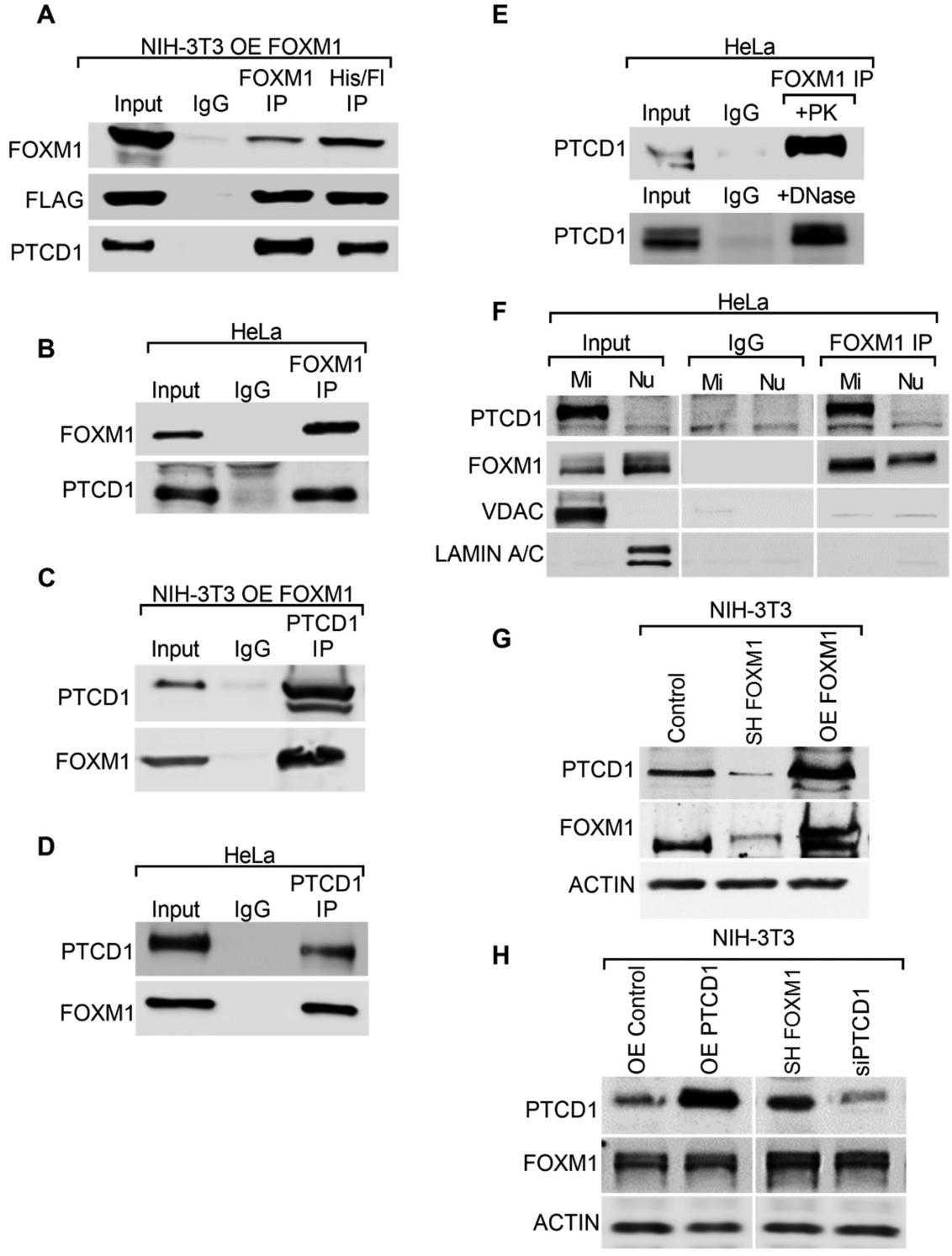

FIGURE 5: FOXM1 and PTCD1 are protein binding partners. (A) PTCD1 in FOXM1 immunoprecipitates. NIH-3T3 cells expressing FOXM1 (*OE FOXM1*), which contains HIS and FLAG tags, were subjected to 2-step affinity chromatography using anti-FLAG and anti-HIS affinity columns. The elutes were analyzed by Western blot using antibodies for FOXM1, FLAG, and PTCD1. Cells incubated with IgG were used as controls. (B) Immunoblots show immunoprecipitation (IP) of endogenous FOXM1 with PTCD1 in HeLa cells. (C, D) FOXM1 in PTCD1 immunoprecipitates. (C) NIH-3T3 cells expressing FOXM1 (*OE FOXM1*) or (D) HeLa cells immunoprecipitated using PTCD1 antibody. Immunoblots show IP of endogenous PTCD1 protein with FOXM1. (E) Proteinase K and DNase treatments do not influence interactions of endogenous FOXM1 with PTCD1. Total wild-type HeLa cell lysates were incubated with 10 µg/ml proteinase K (PK) or DNase for 30 min. FOXM1 IP experiments were performed, and blots were probed with PTCD1 antibodies. (F) FOXM1 and PTCD1 are bound in mitochondrial lysates. FOXM1 or nonspecific isotype-matched IgG was incubated with purified mitochondrial (Mi) and nuclear (Nu) fractions from HeLa cells. Immunoprecipitates were resolved on SDS–PAGE and probed for PTCD1, FOXM1, VDAC (mitochondrial protein), and LAMIN A/C (nuclear protein). (G) FOXM1 directly

(Primers: forward 5′ CGC CGC TAG CAA GCT TGT GAC CAT GTC CGT CCT GAC GCC GCT GCT GCT GCG GGG CTT GAC AGG CTC GGC CCG GCG GCT CCC AGT GCC GCG CGC CAA GAT CCA TTC GTT GGG AT 3′ and reverse 5′ ATC CCA ACG AAT GGA TCT TGG C 3′). To inhibit FOXM1 localization to mitochondria and target FOXM1 to the nucleus, the endogenous FOXM1 MLS was mutated by substituting lysine and arginine amino acids for alanine. (Primers: forward 5′CGG CCA CTG ATT CTC CGA GCA GCG GCG CTG CCC CTT CCT GTT 3′ and reverse 5′ AAC AGG AAG GGG CAG CGC CGC TGC TCG GAG AAT CAG TGG CCG 3′. Forward 5′ CAA ATG GGTATG GCA ACT AGC CCC GCT GCG CCA CTG ATT CTC and reverse 5′ GAG AAT CAG TGG CGC AGC GGG GCT AGT TGC CAT ACC CAT TTG 3′). NIH-3T3, HeLa, and A549 cells were cultured and maintained using standard procedures as described previously (Cheng *et al.*, 2014; Pradhan *et al.*, 2016). Plasmid and siRNA transfection was performed using Lipofectamine 2000 (Invitrogen). For transient knockdown of *FOXM1*, we used siRNAs targeting either ORF (mouse: 5′-GAAAGGAGUUUGUCUUCU C-3′ and human: 5′-GGAAAUGCCAGGCGCUCAAUU-3′) or si*FOXM1*–3′UTR (mouse: 5′-CCAGAUACGUGGAAA GAAUUU-3′ and human: 5′-GCAGAAAGGUUAAGGCACUUU-3′). siRNA against a nontargeting sequence (Invitrogen) was used as control in all experiments. For retroviral-mediated stable knockdown of *FOXM1*, a shRNA targeting 3′UTR of human FOXM1 was used (5′-AAATGTTAGTGGT-GGGTCTGA-3′). Stable cell lines were generated using pMIEG3 retroviral vector, which expresses an enhanced green fluorescent protein (eGFP) when incorporated into the genome (Milewski *et al.*, 2017b). Cells were sorted for GFP. Cells lines generated expressed either *pMIEG3-EV* (CONTROL), *pMIEG3-FOXM1/FLAG* (OE FOXM1), or *pMIEG3:shFOXM1–3′UTR* (SH FOXM1)

Fluorescence immunocytochemistry

Cell lines were seeded onto glass cover slips (1.5 mm), stained with MitoTracker dye (Molecular Probes Invitrogen) at 100 nM, fixed with 2% paraformaldehyde, and permeabilized with 0.2% Triton X-100 in 1% bovine serum albumin for 5 min. Cells were stained with primary antibodies (see Supplemental Table 1) overnight at 4°C. After being washed in PBS, the cells were stained with Alexa Fluor–conjugated secondary antibodies and incubated for 1 h at room temperature, followed by nuclear counterstaining with 4′,6-diamidino-2-phenylindole (DAPI). Cell image analysis to measure subcellular localization of Foxm1 was performed using CellProfiler (Carpenter *et al.*, 2006). The fraction (in percent) of Foxm1 fluorescence signal (mean pixel intensity) localized throughout the cytoplasmic and nuclear cellular compartments was determined using CellProfiler software, which identifies pixel intensities and spatial information segmented by nonnuclear versus nuclear localization within each cell image (Carpenter *et al.*, 2006). Each image was segmented by nuclear localization using DAPI and separated by individual color channels. The images were aligned and measured for object correlation and pixel intensity correlation based on the individual cellular compartments identified.

Measurement of mitochondrial content and mitochondrial membrane potential

Fluorescence-activated cell sorting (FACS) analysis of mitochondria-localized fluorescent dyes was used to assess relative mitochondrial content and mitochondrial membrane potential, with MitoTracker Green FM (MTG) (ThermoFisher) and tetramethylrhodamine methyl ester (TMRM) (Invitrogen), respectively (Brand and Nicholls, 2011; Dingley *et al.*, 2012; De Luca *et al.*, 2015). Cell suspensions were costained with MTG (200 nM) and TMRM (20 nM). Propidium iodide (ThermoFisher) was used to detect dead cells. Stained cells were analyzed using a FACSCanto II flow cytometer (BD FACSCanto II; BD Bioscience, San Jose, CA) as previously described (Cai *et al.*, 2016).

Mitochondrial respiration

Mitochondrial respiration was determined by measuring the oxygen consumption rate (OCR) with a Bioscience Seahorse XF^e-24 extracellular flux analyzer and the XF Cell Mito Stress Test Kit (Agilent). XF24 creates a transient, 500-µl chamber in specialized microplates that allows for the determination of oxygen and proton concentrations in real time. To allow comparison between different experiments, data are expressed as the rate of oxygen consumption in pmol/min or the rate of extracellular acidification in mpH/min, normalized to cell protein in individual wells determined by the Bradford protein assay (Bio-Rad). A density of 80,000 cells per well in a 24-well plate was coated with poly-D-lysine (Sigma) adhesive. The rates of O_2 were determined under basal condition and with the addition of oligomycin (1.5 µM), carbonyl cyanide *p*-(trifluoromethoxy) phenylhydrazone (FCCP) (0.5 µM), rotenone (1 µM) and antimycin A (1 µM). ATP-linked respiration was derived from the difference between OCR at baseline and following oligomycin addition. The difference in OCR between antimycin A and oligomycin represented the amount of oxygen consumed due to proton leak. Maximal OCR was determined by subtracting the OCR after antimycin A addition from the OCR induced by carbonyl cyanide-*p*-trifluoromethoxyphenylhydrazone (FCCP). Finally, the reserve capacity was calculated by the difference between maximal and basal respirations.

Cell counts

Cells were plated at 1×10^5 density. Viable cells were counted at 24, 48, and 72 h time points using a hemocytometer as previously described (Kalin *et al.*, 2008a; Black *et al.*, 2018). Experiments were performed in triplicate and presented as average numbers of cells ± SEM.

Cell cycle analysis

Cell cycle analysis was done as previously described (Cheng *et al.*, 2014; Milewski *et al.*, 2017a). NIH-3T3 cells with stable depletion of FOXM1 transfected with MLS constructs were serum starved for 48 h by using DMEM supplemented with 0.1% fetal bovine serum (FBS). Complete media with 10% FBS was added, and cells were collected after 72 h and stained with Hoechst 33342 (ThermoFisher) for DNA content and 7AAD (eBioscience) for cell viability. Flow cytometry FACS analysis (BD LSRForetessa I; BD Bioscience, San Jose, CA) was used to count cells in G0/G1, S, and G2/M phases of cell cycle.

ETC complex activity assays

Mitochondrial respiratory chain activities for each complex were measured using kits from Mitoscience-Abcam according to the manufacturers' instructions: complex I (ab109721), II (ab109908),

correlates with PTCD1 protein levels. Immunoblots show FOXM1 and PTCD1 protein levels in total cell lysates of NIH-3T3 cells that stably express control, shFOXM1, and OE FOXM1. ACTIN was used as a loading control. (H) Changes in PTCD1 does not affect FOXM1 levels. NIH-3T3 cells were transiently transfected with the indicated constructs. Immunoblots show FOXM1 and PTCD1 protein levels in total lysates of NIH-3T3 cells expressing *OE CONTROL*, *OE PTCD1*, *siCONTROL*, and *siPTCD1*. β -ACTIN was used as a loading control.

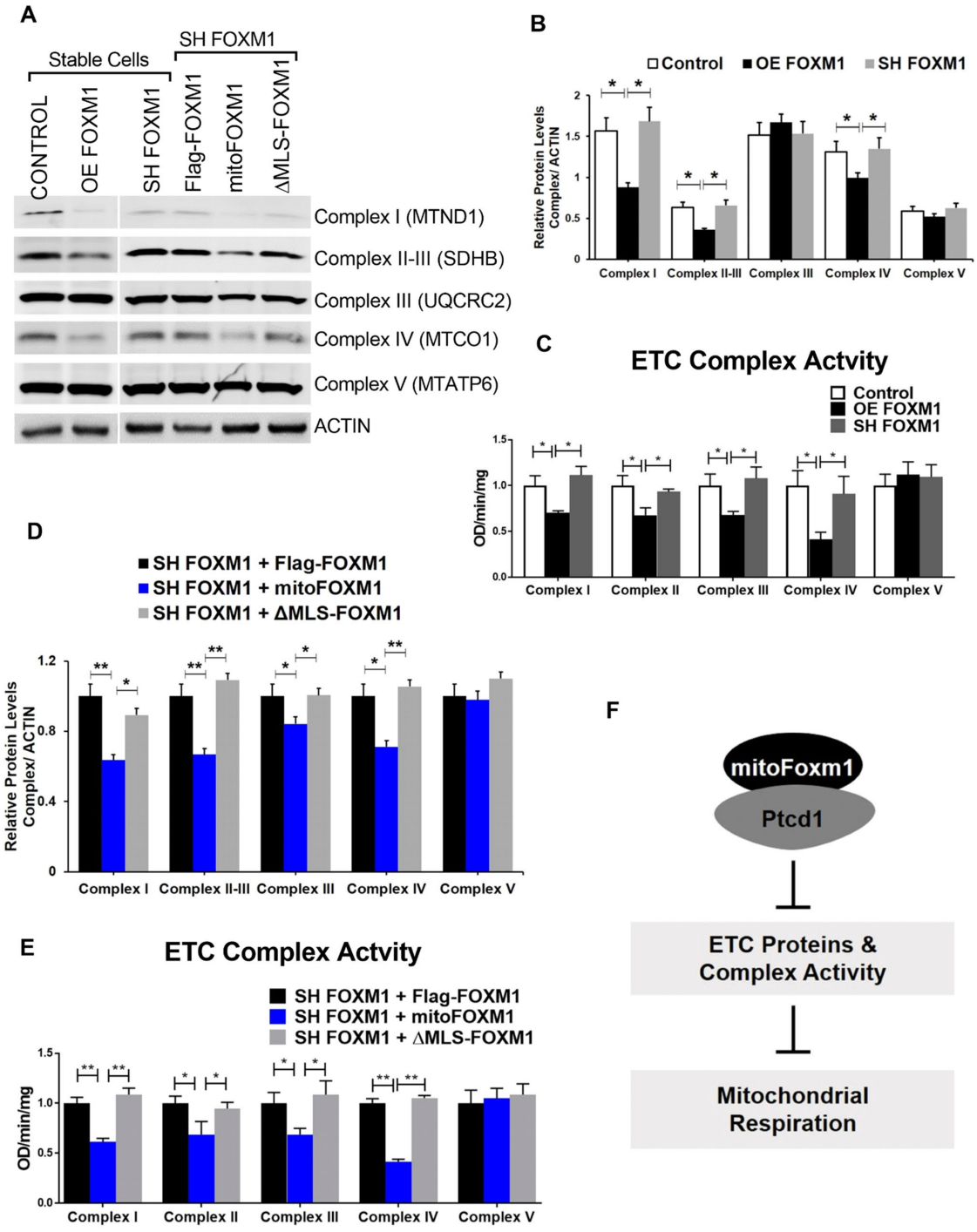

FIGURE 6: Mitochondrial FOXM1 decreases ETC complex protein levels and activity. (A) Western blot analysis of mitochondrial proteins. Total cellular proteins from FOXM1 stable cell lines and *SH FOXM1* cells expressing MLS mutant constructs were probed for proteins from each ETC complex and β-ACTIN as a loading control. MTATP6 indicates protein subunit 6 from ETC complex V; MTCO1 indicates protein subunit 1 from ETC complex IV; UQCRC2 indicates protein subunit 2 from ETC complex III; SDHB indicates protein subunit from ETC complex II; MTND1 indicates protein subunit 1 from ETC complex I. (B) Densitometric quantification of mitochondrial proteins in stable control and OE FOXM1 and SH FOXM1 cell lines. Average MTND1, SDHB, MTCO1, UQCRC2, or MTATP6 levels were normalized to ACTIN. Values are expressed relative to Flag-FOXM1 control. Data represent mean ± SEM from three determinations. Statistical significance is indicated with an asterisk; *$p < 0.05$. (C) Enzymatic activities of respiratory chain complexes in stable control and OE FOXM1 and SH FOXM1 cell lines. The activities of respiratory complexes were investigated by enzymatic assays on complexes I, II, III, IV, and V in mitochondrial or total cell lysates. Activities are expressed as OD absorbance/min/mg total protein or mitochondrial protein. Data represent mean ± SEM from experiments in triplicate. Statistical significance is indicated with an asterisk; *$p < 0.05$. (D) Densitometric quantification of mitochondrial proteins in *SH FOXM1* cells expressing MLS mutant constructs. Average MTND1, SDHB, MTCO1, UQCRC2, or MTATP6 levels were normalized to ACTIN. Values are expressed as relative to Flag-FOXM1 control. Data represent mean ± SEM

from three determinations. Statistical significance is indicated with an asterisk; *$p < 0.05$, **$p < 0.01$. (E) Enzymatic activities of respiratory chain complexes in *SH FOXM1* cells expressing MLS mutant constructs. The activities of respiratory complexes were investigated by enzymatic assays on complexes I, II, III, IV, and V in mitochondrial or total cell lysates. Activities are expressed as OD absorbance/min/mg total protein or mitochondrial protein. Data represent mean ± SEM from experiments in triplicate. Statistical significance is indicated with an asterisk; *$p < 0.05$, **$p < 0.01$. (F) Schematic diagram. FOXM1 translocates into the mitochondria, interacts with PTCD, and inhibits mitochondrial respiration.

IV (ab109911), and V (ab109714). Briefly, capture antibodies specific for each mitochondrial respiratory chain complex are precoated in each well of a 96-well microplate. Cell cultures or isolated mitochondria are added to the microplate wells, which have been precoated with a specific capture antibody. After the target has been immobilized in the well, the complex activity is determined by following the oxidation and reduction of complex-specific substrates and a dye. The absorbance is measured at specific optical densities (OD) using a spectrophotometer. Complex III activity was measured using a kit from BioVision (K520) according to the manufacturer's instructions. Briefly, this kit for complex III activity assay is based on the reduction of cytochrome *c* through the activity of complex III. The absorbance of reduced cytochrome *c* is measured at 550 nm in isolated mitochondria.

Statistics

Statistical significance differences in measured variables between experimental and control groups were assessed by Student's *t* test (2-tailed) or one-way analysis of variance (ANOVA) with Bonferronni test. *P* values < 0.05 were considered significant. Values for all measurements were expressed as the mean ± SD or as the mean ± standard error of mean. Statistical analysis was performed, and data were graphically displayed using GraphPad Prism v.5.0 for Windows (GraphPad Software).

ACKNOWLEDGMENTS

This work was supported by National Institutes of Health (NIH) grants T32-HR007752 (M.B.), R01HL132849 (T.V.K.), R56HL126660 (T.V.K.), R01 CA142724 (T.V.K.), RO1HL84151 (V.V.K.), and RO1HL123490 (V.V.K.).

REFERENCES

Asin-Cayuela J, Gustafsson CM (2007). Mitochondrial transcription and its regulation in mammalian cells. Trends Biochem Sci 32, 111–117.

Balli D, Ren X, Chou FS, Cross E, Zhang Y, Kalinichenko VV, Kalin TV (2012). Foxm1 transcription factor is required for macrophage migration during lung inflammation and tumor formation. Oncogene 31, 3875–3888.

Balli D, Ustiyan V, Zhang Y, Wang IC, Masino AJ, Ren X, Whitsett JA, Kalinichenko VV, Kalin TV (2013). Foxm1 transcription factor is required for lung fibrosis and epithelial-to-mesenchymal transition. EMBO J 32, 231–244.

Balli D, Zhang Y, Snyder J, Kalinichenko VV, Kalin TV (2011). Endothelial cell-specific deletion of transcription factor FoxM1 increases urethane-induced lung carcinogenesis. Cancer Res 71, 40–50.

Black M, Milewski D, Le T, Ren X, Xu Y, Kalinichenko VV, Kalin TV (2018). FOXF1 inhibits pulmonary fibrosis by preventing CDH2-CDH11 cadherin switch in myofibroblasts. Cell Rep 23, 442–458.

Brand MD, Nicholls DG (2011). Assessing mitochondrial dysfunction in cells. Biochem J 435, 297–312.

Cai Y, Balli D, Ustiyan V, Fulford L, Hiller A, Misetic V, Zhang Y, Paluch AM, Waltz SE, Kasper S, Kalin TV (2013). Foxm1 expression in prostate epithelial cells is essential for prostate carcinogenesis. J Biol Chem 288, 22527–22541.

Cai Y, Bolte C, Le T, Goda C, Xu Y, Kalin TV, Kalinichenko VV (2016). FOXF1 maintains endothelial barrier function and prevents edema after lung injury. Sci Signal 9, ra40.

Carbognin E, Betto RM, Soriano ME, Smith AG, Martello G (2016). Stat3 promotes mitochondrial transcription and oxidative respiration during maintenance and induction of naive pluripotency. EMBO J 35, 618–634.

Carpenter AE, Jones TR, Lamprecht MR, Clarke C, Kang IH, Friman O, Guertin DA, Chang JH, Lindquist RA, Moffat J, *et al.* (2006). CellProfiler: image analysis software for identifying and quantifying cell phenotypes. Genome Biol 7, R100.

Cheng X-H, Black M, Ustiyan V, Le T, Fulford L, Sridharan A, Medvedovic M, Kalinichenko VV, Whitsett JA, Kalin TV (2014). SPDEF inhibits prostate carcinogenesis by disrupting a positive feedback loop in regulation of the Foxm1 oncogene. PLoS Genet 10, e1004656.

Claros MG (1995). MitoProt, a Macintosh application for studying mitochondrial proteins. Comput Appl Biosci 11, 441–447.

Claros MG, Vincens P (1996). Computational method to predict mitochondrially imported proteins and their targeting sequences. Eur J Biochem 241, 779–786.

Costa RH, Kalinichenko VV, Major ML, Raychaudhuri P (2005). New and unexpected: forkhead meets ARF. Curr Opin Genet Dev 15, 42–48.

Cui J, Shi M, Xie D, Wei D, Jia Z, Zheng S, Gao Y, Huang S, Xie K (2014). FOXM1 promotes the Warburg effect and pancreatic cancer progression via transactivation of LDHA expression. Clin Cancer Res 20, 2595–2606.

Cunniff B, Benson K, Stumpff J, Newick K, Held P, Taatjes D, Joseph J, Kalyanaraman B, Heintz NH (2013). Mitochondrial-targeted nitroxides disrupt mitochondrial architecture and inhibit expression of Peroxiredoxin 3 and FOXM1 in malignant mesothelioma cells. J Cell Physiol 228, 835–845.

Davies SMK, Lopez Sanchez MIG, Narsai R, Shearwood A-MJ, Razif MFM, Small ID, Whelan J, Rackham O, Filipovska A (2012). MRPS27 is a pentatricopeptide repeat domain protein required for the translation of mitochondrially encoded proteins. FEBS Lett 586, 3555–3561.

De Luca A, Fiorillo M, Peiris-Pagès M, Ozsvari B, Smith DL, Sanchez-Alvarez R, Martinez-Outschoorn UE, Cappello AR, Pezzi V, Lisanti MP, Sotgia F (2015). Mitochondrial biogenesis is required for the anchorage-independent survival and propagation of stem-like cancer cells. Oncotarget 6, 14777–14795.

Dingley S, Chapman KA, Falk MJ (2012). Fluorescence-activated cell sorting analysis of mitochondrial content, membrane potential, and matrix oxidant burden in human lymphoblastoid cell lines. Methods Mol Biol 837, 231–239.

Everts HB, Berdanier CD (2002). Regulation of mitochondrial gene expression by retinoids. IUBMB Life 54, 45–49.

Falkenberg M, Larsson N-G, Gustafsson CM (2007). DNA replication and transcription in mammalian mitochondria. Annu Rev Biochem 76, 679–699.

Frezza C, Cipolat S, Scorrano L (2007). Organelle isolation: functional mitochondria from mouse liver, muscle and cultured filroblasts. Nat Protocols 2, 287–295.

Kalin TV, Meliton L, Meliton AY, Zhu X, Whitsett JA, Kalinichenko VV (2008a). Pulmonary mastocytosis and enhanced lung inflammation in mice heterozygous null for the Foxf1 gene. Am J Respir Cell Mol Biol 39, 390–399.

Kalin TV, Ustiyan V, Kalinichenko VV (2011a). Multiple faces of FoxM1 transcription factor. Cell Cycle 10, 396–405.

Kalin TV, Ustiyan V, Kalinichenko VV (2011b). Multiple faces of FoxM1 transcription factor: lessons from transgenic mouse models. Cell Cycle 10, 396–405.

Kalin TV, Wang I-C, Meliton L, Zhang Y, Wert SE, Ren X, Snyder J, Bell SM, Graf L, Whitsett JA, Kalinichenko VV (2008b). Forkhead Box m1 transcription factor is required for perinatal lung function. Proc Natl Acad Sci 105, 19330–19335.

Kalin TV, Wang IC, Ackerson TJ, Major ML, Detrisac CJ, Kalinichenko VV, Lyubimov A, Costa RH (2006). Increased levels of the FoxM1 transcription factor accelerate development and progression of prostate carcinomas in both TRAMP and LADY transgenic mice. Cancer Res 66, 1712–1720.

Kalinichenko VV, Kalin TV (2015). Is there potential to target FOXM1 for "undruggable" lung cancers? Expert Opin. Ther Targets 19, 865–867.

Kalinichenko VV, Major M, Wang X, Petrovic V, Kuechle J, Yoder HM, Shin B, Datta A, Raychaudhuri P, Costa RH (2004). Forkhead Box m1b transcription factor is essential for development of hepatocellular carcinomas and is negatively regulated by the p19ARF tumor suppressor. Genes Dev 18, 830–850.

Laker RC, Xu P, Ryall KA, Sujkowski A, Kenwood BM, Chain KH, Zhang M, Royal MA, Hoehn KL, Driscoll M, *et al.* (2014). A novel MitoTimer reporter gene for mitochondrial content, structure, stress, and damage in vivo. J Biol Chem 289, 12005–12015.

Laoukili J, Kooistra MRH, Brás A, Kauw J, Kerkhoven RM, Morrison A, Clevers H, Medema RH (2005). FoxM1 is required for execution of the mitotic programme and chromosome stability. Nat Cell Biol 7, 126–136.

Leigh-Brown S, Enriquez J, Odom D (2010). Nuclear transcription factors in mammalian mitochondria. Genome Biol 11, 215.

Ma RYM, Tong THK, Cheung AMS, Tsang ACC, Leung WY, Yao K-M (2005). Raf/MEK/MAPK signaling stimulates the nuclear translocation and transactivating activity of FOXM1c. J Cell Sci 118, 795–806.

Maachani UB, Shankavaram U, Kramp T, Tofilon PJ, Camphausen K, Tandle AT (2016). FOXM1 and STAT3 interaction confers radioresistance in glioblastoma cells. Oncotarget 7, 77365–77377.

Milewski D, Balli D, Ustiyan V, Le T, Dienemann H, Warth A, Breuhahn K, Whitsett JA, Kalinichenko VV, Kalin TV (2017a). FOXM1 activates AGR2 and causes progression of lung adenomas into invasive mucinous adenocarcinomas. PLoS Genet 13, e1007097.

Milewski D, Pradhan A, Wang X, Cai Y, Le T, Turpin B, Kalinichenko VV, Kalin TV (2017b). FoxF1 and FoxF2 transcription factors synergistically promote rhabdomyosarcoma carcinogenesis by repressing transcription of p21(Cip1) CDK inhibitor. Oncogene 36, 850–862.

Myatt SS, Lam EW, (2007). The emerging roles of forkhead box (Fox) proteins in cancer. Nat Rev Cancer 7, 847–859.

Nunnari J, Suomalainen A (2012). Mitochondria: in sickness and in health. Cell 148, 1145–1159.

Park HJ, Carr JR, Wang Z, Nogueira V, Hay N, Tyner AL, Lau LF, Costa RH, Raychaudhuri P (2009). FoxM1, a critical regulator of oxidative stress during oncogenesis. EMBO J 28, 2908–2918.

Park HJ, Costa RH, Lau LF, Tyner AL, Raychaudhuri P (2008). Anaphase-promoting complex/cyclosome-Cdh1-mediated proteolysis of the Forkhead Box M1 transcription factor is critical for regulated entry into S phase. Mol Cell Biol 28, 5162–5171.

Perks KL, Rossetti G, Kuznetsova I, Hughes LA, Ermer JA, Ferreira N, Busch JD, Rudler DL, Spahr H, Schondorf T, *et al.* (2018). PTCD1 is required for 16S rRNA maturation complex stability and mitochondrial ribosome assembly. Cell Rep 23, 127–142.

Pradhan A, Ustiyan V, Zhang Y, Kalin TV, Kalinichenko VV (2016). Forkhead transcription factor FoxF1 interacts with Fanconi anemia protein complexes to promote DNA damage response. Oncotarget 7, 1912–1926.

Rackham O, Davies SMK, Shearwood A-MJ, Hamilton KL, Whelan J, Filipovska A (2009). Pentatricopeptide repeat domain protein 1 lowers the levels of mitochondrial leucine tRNAs in cells. Nucleic Acids Res 37, 5859–5867.

Ren X, Zhang Y, Snyder J, Cross ER, Shah TA, Kalin TV, Kalinichenko VV (2010). Forkhead Box M1 transcription factor is required for macrophage recruitment during liver repair. Mol Cell Biol 30, 5381–5393.

Schild C, Hahn D, Schaller A, Jackson CB, Rothen-Rutishauser B, Mirkovitch J, Nuoffer J-M (2014). Mitochondrial leucine tRNA level and PTCD1 are regulated in response to leucine starvation. Amino Acids 46, 1775–1783.

She H, Yang Q, Shepherd K, Smith Y, Miller G, Testa C, Mao Z (2011). Direct regulation of complex I by mitochondrial MEF2D is disrupted in a mouse model of Parkinson disease and in human patients. J Clin Invest 121, 930–940.

Shukla S, Milewski D, Pradhan A, Rama N, Rice K, Le T, Flick MJ, Vaz S, Zhao X, Setchell KD, *et al.* (2019). The FOXM1 inhibitor RCM-1 decreases carcinogenesis and nuclear beta-catenin. Mol Cancer Ther 18, 1217–1229.

Sievers F, Wilm A, Dineen D, Gibson TJ, Karplus K, Li W, Lopez R, McWilliam H, Remmert M, Söding J, *et al.* (2011). Fast, scalable generation of high-quality protein multiple sequence alignments using Clustal Omega. Mol Syst Biol 7, 539.

Sun L, Ren X, Wang IC, Pradhan A, Zhang Y, Flood HM, Han B, Whitsett JA, Kalin TV, Kalinichenko VV (2017). The FOXM1 inhibitor RCM-1 suppresses goblet cell metaplasia and prevents IL-13 and STAT6 signaling in allergen-exposed mice. Sci Signal 10, eaai8583.

Suzuki T, Nagao A, Suzuki T (2011). Human mitochondrial tRNAs: biogenesis, function, structural aspects, and diseases. Annu Rev Genet 45, 299–329.

Szczepanek K, Lesnefsky EJ, Larner AC (2012). Multi-tasking: nuclear transcription factors with novel roles in the mitochondria. Trends Cell Biol 22, 429–437.

Taylor RW, Pyle A, Griffin H, Blakely EL, Duff J, He L, Smertenko T, Alston CL, Neeve VC, Best A (2014). Use of whole-exome sequencing to determine the genetic basis of multiple mitochondrial respiratory chain complex deficiencies. J Am Med Assoc 312, 68–77.

Teh M-T, Wong S-T, Neill GW, Ghali LR, Philpott MP, Quinn AG (2002). FOXM1 is a downstream target of Gli1 in basal cell carcinomas. Cancer Res 62, 4773–4780.

Vander Heiden MG, Cantley LC, Thompson CB (2009). Understanding the Warburg effect: the metabolic requirements of cell proliferation. Science 324, 1029.

Wang I-C, Chen Y-J, Hughes D, Petrovic V, Major ML, Park HJ, Tan Y, Ackerson T, Costa RH (2005). Forkhead Box M1 regulates the transcriptional network of genes essential for mitotic progression and genes encoding the SCF (Skp2-Cks1) ubiquitin ligase. Mol Cell Biol 25, 10875–10894.

Wang IC, Meliton L, Tretiakova M, Costa RH, Kalinichenko VV, Kalin TV (2008). Transgenic expression of the forkhead box M1 transcription factor induces formation of lung tumors. Oncogene 27, 4137–4149.

Wang IC, Snyder J, Zhang Y, Lander J, Nakafuku Y, Lin J, Chen G, Kalin TV, Whitsett JA, Kalinichenko VV (2012). Foxm1 mediates cross talk between Kras/mitogen-activated protein kinase and canonical Wnt pathways during development of respiratory epithelium. Mol Cell Biol 32, 3838–3850.

Wang IC, Ustiyan V, Zhang Y, Cai Y, Kalin TV, Kalinichenko VV (2014). Foxm1 transcription factor is required for the initiation of lung tumorigenesis by oncogenic Kras(G12D.). Oncogene 33, 5391–5396.

Wegrzyn J, Potla R, Chwae Y-J, Sepuri NBV, Zhang Q, Koeck T, Derecka M, Szczepanek K, Szelag M, Gornicka A, *et al.* (2009). Function of mitochondrial Stat3 in cellular respiration. Science 323, 793–797.

Weiler SME, Pinna F, Wolf T, Lutz T, Geldiyev A, Sticht C, Knaub M, Thomann S, Bissinger M, Wan S, *et al.* (2017). Induction of chromosome instability by activation of Yes-associated protein and Forkhead Box M1 in liver cancer. Gastroenterology 152, 2037–2051.e2022.

Zhang J, Nuebel E, Wisidagama DRR, Setoguchi K, Hong JS, Van Horn CM, Imam SS, Vergnes L, Malone CS, Koehler CM, Teitell MA (2012). Measuring energy metabolism in cultured cells, including human pluripotent stem cells and differentiated cells. Nat Protoc 7, doi: 10.1038/nprot.2012.1048.

Zhang Y, Zhang N, Dai B, Liu M, Sawaya R, Xie K, Huang S (2008). FoxM1B transcriptionally regulates vascular endothelial growth factor expression and promotes the angiogenesis and growth of glioma cells. Cancer Res 68, 8733–8742.